

Quantum triangular ice in the easy-axis ferromagnetic phase

S. A. Owerre^{1,2,*}

¹*African Institute for Mathematical Sciences, 6 Melrose Road, Muizenberg, Cape Town 7945, South Africa.*[†]

²*Perimeter Institute for Theoretical Physics, 31 Caroline St. N., Waterloo, Ontario N2L 2Y5, Canada.*

We use spin wave theory to investigate the ground state properties of the Z_2 -invariant quantum XXZ model on the triangular lattice in the ferromagnetic phase. The Hamiltonian comprises nearest and next-nearest-neighbour Ising couplings, external magnetic fields, and a Z_2 -invariant ferromagnetic coupling. We show that quantum fluctuations are suppressed in this system, hence linear spin wave theory gives reasonable estimates of the ground state thermodynamic properties. Our results show that, at half-filling (zero magnetic fields), the spontaneous breaking of Z_2 symmetry leads to a ferromagnetic phase whose energy spectrum is gapped at all excitations with a *maxon* dispersion at $\mathbf{k} = 0$. This is in sharp contrast to rotational invariant systems with a vanishing *phonon* dispersion. We show that the $\mathbf{k} = 0$ mode enhances the estimated values of the thermodynamic quantities. We obtain the trends of the particle density and the condensate fraction. The density of states and the dynamical structure factors exhibit fascinating peaks at unusual wave vectors, which should be of interest.

PACS numbers: 75.10.Jm, 75.30.Ds, 05.30.Jp, 75.40.Gb

Introduction— Quantum spin ice (QSI) on three-dimensional pyrochlore lattice has become the subject of intense research in recent years.^{1–3} In this system, the spin ordering at the vertices of the pyrochlore lattice, that is two-in, two-out, is reminiscent of hydrogen atoms in water ice. Competing interactions between frustrated spins give rise to fascinating physics with rich quantum phases. Huang, Chan and Hermele⁴ recently proposed an alternative simplified Hamiltonian that captures the physics of QSI on three-dimensional pyrochlore lattice. In the presence of a [111] crystallographic field, the spin configurations exhibit an ordering which can be mapped onto a two-dimensional kagome lattice.⁵ The Hamiltonian, however, retains the same form as the Huang, Chan and Hermele model. Recently, Carrasquilla *et al.*,⁵ have uncovered the phase diagram of this model on the kagome lattice by Quantum Monte Carlo (QMC) simulations. The Hamiltonian studied by Carrasquilla *et al.*,⁵ is termed *Quantum Kagome Ice* and it has the form

$$H = -\frac{J_{\pm\pm}}{2} \sum_{\langle lm \rangle} (S_l^+ S_m^+ + S_l^- S_m^-) + J_z \sum_{\langle lm \rangle} S_l^z S_m^z - h_z \sum_l S_l^z, \quad (1)$$

where $S_l^\pm = S_l^x \pm iS_l^y$ are the raising and the lowering spin operators respectively. In accordance with previous terminology, the term *Quantum Triangular Ice* refers to the study of Eq. (1) on the triangular lattice. Here, $J_z > 0$ is the frustrated nearest-neighbour (nn) Ising coupling, and $J_{\pm\pm} > 0$ is the unfrustrated Z_2 -invariant easy-axis ferromagnetic coupling. The sign of $J_{\pm\pm}$ is immaterial by virtue of the unitary transformation $S_{lm}^\pm \rightarrow \pm iS_{lm}^\pm$.

The crucial difference between the U(1)-invariant XXZ model^{6–12} and Eq. (1) is that the ferromagnetic interaction in the former is easy-plane and has a unique sign for non-bipartite lattices, whereas in the latter, the ferromagnetic interaction is easy-axis and the sign is im-

material, which results in a Z_2 -invariant Hamiltonian in the x - y plane. Thus, Eq. (1) cannot be mapped onto a U(1)-invariant XXZ model (hard-core boson) on non-bipartite lattices, whereas for bipartite lattices, Eq. (1) is related to the U(1)-invariant counterpart by a simple spin flip. QMC simulations of Carrasquilla *et al.*⁵ on the kagome lattice uncovered three distinct phases, which include the unconventional disordered magnetized lobes for small $\pm h_z$ and $J_{\pm\pm}/J_z < 0.5$, and it is believed to be a candidate for Quantum Spin Liquid (QSL) state, enabling the search for two-dimensional QSL within a class of pyrochlore QSI materials. The remaining two phases are the S_x and the S_z ferromagnetic ordered phases for small and large h_z respectively.

We have provided an analytical explanation of the QMC results using spin wave theory on the kagome lattice.¹³ Remarkably, we observed that the average spin-deviation operator $\langle n_l \rangle = \langle b_l^\dagger b_l \rangle$ is very small in *Quantum Kagome Ice*, *i.e.*, quantum fluctuations are suppressed. Hence, we were able to capture a broad trend of the quantum phases uncovered by QMC simulations.⁵ We have also obtained the complete phase diagram of Eq. (1) on the triangular lattice (*Quantum Triangular Ice*), using the semiclassical large- S expansion.¹⁴ In the case of triangular lattice, there is an additional phase at $h_z = 0$ and $J_z \rightarrow \infty$. This phase is selected by quantum fluctuations via order-by-disorder mechanism and it is called a *ferrosolid* state — a state similar to a *supersolid* state in the U(1)-invariant XXZ model,^{6–10} but exhibits broken translational and Z_2 symmetries. It also appears adjacent to the unconventional disordered magnetized lobes for small $\pm h_z$. Again, spin wave theory provides an accurate picture of the quantum phases. The XY limit of this model on both lattices has also been analyzed using spin wave theory and QMC.¹⁵

In this paper, we explore the ground state properties of the easy-axis ferromagnetic phase of this model on the triangular lattice. A related U(1)-invariant XXZ model

in the superfluid phase has been studied previously on the triangular lattice, using series expansion methods¹¹ and spin wave theory.¹² The present model has not been studied in the ferromagnetic phase. The study of this model has some physical relevance since many magnetic materials are ferromagnets. This includes the unconventional CeRh₃B₂, which has been studied by many authors.¹⁶ The ferromagnetic XY coupling also plays a prominent role in the experimental realization of hard-core bosons in ultracold atoms on quantum optical lattices.^{17,18} Hence, it is expedient to understand the ferromagnetic nature of the Z_2 -invariant model, as it might be applicable to these systems. We will consider a more general Hamiltonian given by

$$H = -\frac{J_{\pm\pm}}{2} \sum_{\langle lm \rangle} (S_l^+ S_m^+ + S_l^- S_m^-) + \sum_{lm} J_{l,m} S_l^z S_m^z - h_z \sum_l S_l^z - h_x \sum_l S_l^x, \quad (2)$$

where $J_{l,m} = J_z$ on the nn sites and $J_{l,m} = J'_z$ on the next-nearest-neighbour (nnn) sites. The external magnetic fields are introduced to enable the calculation of parallel and longitudinal magnetizations. The Z_2 symmetry of Eq. (2) at $h_x = 0$ is synonymous with the fact that the total S_z is not conserved.

In this model, spin wave theory is exact at the Heisenberg point $J'_z = h_{x,z} = 0$ and $J_z = J_{\pm\pm} = J$. The exact ground state in this limit is a ferromagnet along the x -direction. The excitation spectrum, however, exhibits no soft (Goldstone) modes at $\mathbf{k} = 0$ and the average spin-deviation is not divergent at finite temperature. Hence, the discrete Z_2 symmetry is spontaneously broken even at finite temperature, thus Mermin-Wagner theorem¹⁹ is not applicable. This unusual feature is obviously absent in rotational invariant systems. Away from the Heisenberg point, the average spin-deviation $\langle n_l \rangle$ does not exceed 0.025 for all parameter regimes considered at half-filling $h_{x,z} = 0$. Thus, spin wave theory gives a very good description of the system. We calculate the excitation spectrum $\epsilon(\mathbf{k})$, the density of states, and the static structure factors $S^{zz}(\mathbf{k})$ and $S^{\pm}(\mathbf{k})$. We also calculate the particle density and the non-divergent condensate fraction at $\mathbf{k} = 0$. In contrast to the $U(1)$ -invariant model, with a phonon dispersion near $\mathbf{k} = 0$,^{11,12} the spectrum of the Z_2 -invariant model exhibits a *maxon* dispersion near $\mathbf{k} = 0$ with a gap of $\Delta \propto \sqrt{J_{\pm\pm}(J_z + J'_z + J_{\pm\pm})}$ at half-filling ($h_{x,z} = 0$). We see that the gap does not vanish for $J_{\pm\pm} \neq 0$. For fixed $J'_z, J_{\pm\pm}$ and varying J_z , we observe well-defined roton minima at some points inside the Brillouin zone. The spectrum also exhibits some profound flat mode at some paths of the Brillouin zone and the gap at the Brillouin zone corners $\mathbf{K} = (\pm 4\pi/3, 0)$ vanishes at $J'_z = J_{\pm\pm} - J_z/2$. Thus, for $J'_z = 0$ the transition between the easy-axis ferromagnet and the *ferrosolid* occurs at $J_z = 2J_{\pm\pm}$, which recovers the result obtained in the $U(1)$ -invariant XXZ model.⁶ However, spin wave theory gives a better description of the present model. The static

structure factors exhibit some distinctive features with sharp peaks at the minima of the energy spectra and no discontinuity in the entire Brillouin zone. Likewise, the density of states exhibit interesting features with peaks at various energies.

Linear spin wave theory-. We now consider the anisotropic Hamiltonian in Eq. (2) in the easy-axis ferromagnetic phase. At the Heisenberg point $J'_z = h_{x,z} = 0$ and $J_z = J_{\pm\pm} = J$, the resulting Hamiltonian can be written as

$$H = J \sum_{\langle lm \rangle} -S_l^x S_m^x + \frac{1}{2} (S_l^+ S_m^- + S_l^- S_m^+). \quad (3)$$

We have chosen x -quantization axis, hence $S_l^{\pm} = S_l^z \pm iS_l^y$. For bipartite lattices, Eq. (3) can be transformed to $SU(2)$ Heisenberg ferromagnet by a π -rotation about the x -axis on one sublattice, *i.e.*, $S_m^x \rightarrow S_m^x$, $S_m^{\pm} \rightarrow -S_m^{\pm}$. For non-bipartite lattices, such rotation cannot be performed, thus Eq. (3) differs from the $SU(2)$ -invariant Heisenberg ferromagnet, and exhibits $Z_2 \times U(1)$ symmetry with $U(1)$ symmetry in the z - y plane and Z_2 symmetry in the x -axis. The easy-axis ferromagnetic ordered state results from the spontaneous breaking of Z_2 symmetry along the x -axis, $\langle S_x \rangle \neq 0$ and $\langle S_{zy} \rangle = 0$. Thus, for spin-1/2, the state $|\psi_{FM}\rangle = \prod_l |S_l^x = \uparrow\rangle$ is an exact eigenstate of Eq. (3) with $\mathcal{E}_{MF} = -3JNS^2$, and $\langle S_x \rangle = S$. As we will show, the resulting excitation above this ground state has a gapped quadratic dispersing mode near $\mathbf{k} = 0$, signifying no Goldstone mode due to the absence of a complete continuous symmetry. This is in sharp contrast to the superfluid phase with broken $U(1)$ symmetry in the x - y plane $\langle S_{xy} \rangle \neq 0$ and a gapless linear excitation at $\mathbf{k} = 0$.

For the anisotropic model, the mean field energy in the ferromagnetic phase is given by

$$\mathcal{E}_{MF}(\theta) = 3NS^2(\lambda_{1z} + \lambda_{2z} - h/3), \quad (4)$$

where N is the total number of sites and

$$\lambda_{1z} = J_z \cos^2 \theta - J_{\pm\pm} \sin^2 \theta; \quad \lambda_{2z} = J'_z \cos^2 \theta; \quad (5)$$

$$h = h_z \cos \theta + h_x \sin \theta. \quad (6)$$

The minimization of the mean field energy with respect to θ yields

$$h_z - 6\mathcal{J} \cos \vartheta = h_x \cot \vartheta, \quad (7)$$

where ϑ is the angle that minimizes Eq. (4) and $\mathcal{J} = (J_z + J'_z + J_{\pm\pm})$. We can eliminate h_x from Eq. (4) using Eq. (7), the classical energy becomes

$$\mathcal{E}_{MF}(\vartheta) = 3NS^2[\mathcal{J} \sin^2 \vartheta + J_z + J'_z - h_z \sec \vartheta/3]. \quad (8)$$

It should be noted that ϑ is a function of h_x . At $h_x = 0$, the solution of Eq. (7) gives $\cos \vartheta_0 = h_z/h_c$, where $h_c = 6\mathcal{J}$ is the critical field above which the spins are fully polarized along the z -direction. The corresponding classical energy is given by

$$\mathcal{E}_{MF}(\vartheta_0) = -3NS^2[\mathcal{J} \cos^2 \vartheta_0 + J_{\pm\pm}]. \quad (9)$$

For $h_x \neq 0$, the mean field energy is obtained perturbatively for small h_x ,

$$\mathcal{E}_{MF}(\vartheta) = \mathcal{E}_{MF}(h_x = 0) + h_x \left. \frac{\partial \mathcal{E}_{MF}(\vartheta)}{\partial h_x} \right|_{h_x=0} + \dots, \quad (10)$$

where $\mathcal{E}_{MF}(h_x = 0) = \mathcal{E}_{MF}(\vartheta = \vartheta_0)$. We perform spin wave theory in the usual way, by rotating the coordinate about the y -axis in order to align the spins along the selected direction of the magnetization.

$$\begin{aligned} S_l^x &= S_l'^x \cos \theta + S_l'^z \sin \theta, \\ S_l^y &= S_l'^y, \\ S_l^z &= -S_l'^x \sin \theta + S_l'^z \cos \theta. \end{aligned} \quad (11)$$

Next, we express the rotated coordinates in terms of the linearized Holstein Primakoff (HP) transform.

$$\begin{aligned} S_l'^z &= S - b_l^\dagger b_l, \\ S_l'^y &= i\sqrt{\frac{S}{2}} (b_l^\dagger - b_l), \\ S_l'^x &= \sqrt{\frac{S}{2}} (b_l^\dagger + b_l). \end{aligned} \quad (12)$$

The truncation of the HP transformation at linear order is guaranteed provided the average spin-deviation operator $\langle n_l \rangle = \langle b_l^\dagger b_l \rangle$ is small. Indeed, $\langle n_l \rangle$ is small in the present model, hence linear spin wave theory is suitable for the description of this system. Taking the magnetic fields, $h_{x,z}$, to be of order S and keeping only the quadratic terms, the resulting bosonic Hamiltonian can be diagonalized by the Bogoliubov transformation,

$$b_{\mathbf{k}} = u_{\mathbf{k}} \alpha_{\mathbf{k}} - v_{\mathbf{k}} \alpha_{-\mathbf{k}}^\dagger, \quad (13)$$

where $u_{\mathbf{k}}^2 - v_{\mathbf{k}}^2 = 1$, one finds that the resulting Hamiltonian is diagonalized by

$$u_{\mathbf{k}}^2 = \frac{1}{2} \left(\frac{A_{\mathbf{k}}(\vartheta)}{\omega_{\mathbf{k}}(\vartheta)} + 1 \right); \quad v_{\mathbf{k}}^2 = \frac{1}{2} \left(\frac{A_{\mathbf{k}}(\vartheta)}{\omega_{\mathbf{k}}(\vartheta)} - 1 \right), \quad (14)$$

with $\omega_{\mathbf{k}}(\vartheta) = \sqrt{A_{\mathbf{k}}^2(\vartheta) - B_{\mathbf{k}}^2(\vartheta)}$. The diagonal Hamiltonian yields

$$H = S \sum_{\mathbf{k}} \omega_{\mathbf{k}}(\vartheta) \left(\alpha_{\mathbf{k}}^\dagger \alpha_{\mathbf{k}} + \alpha_{-\mathbf{k}}^\dagger \alpha_{-\mathbf{k}} \right). \quad (15)$$

The excitation of the quasiparticles is given by

$$\epsilon_{\mathbf{k}}(\vartheta) = 2S\omega_{\mathbf{k}}(\vartheta) = 2S\sqrt{A_{\mathbf{k}}^2(\vartheta) - B_{\mathbf{k}}^2(\vartheta)}, \quad (16)$$

while the spin wave ground state energy is given by

$$\mathcal{E}_{SW}(\vartheta) = \mathcal{E}_{MF}(\vartheta) + S \sum_{\mathbf{k}} [\omega_{\mathbf{k}}(\vartheta) - \mathcal{E}_{lo}(\vartheta)], \quad (17)$$

where

$$A_{\mathbf{k}}(\vartheta) = \mathcal{E}_{lo}(\vartheta) + 3J_{\pm\pm}\gamma_{\mathbf{k}} + B_{\mathbf{k}}(\vartheta); \quad (18)$$

$$B_{\mathbf{k}}(\vartheta) = \frac{3}{2} (\bar{g}_{\mathbf{k}}(\vartheta) + g_{\mathbf{k}}(\vartheta)); \quad (19)$$

$$\mathcal{E}_{lo}(\vartheta) = -3(J_z + J'_z) + h_z \sec \vartheta/2, \quad (20)$$

$$\bar{g}_{\mathbf{k}}(\vartheta) = (J_z + J_{\pm\pm}) \sin^2 \vartheta \gamma_{\mathbf{k}} - 2J_{\pm\pm} \gamma_{\mathbf{k}}, \quad (21)$$

$$g_{\mathbf{k}}(\vartheta) = J'_z \sin^2 \vartheta \bar{\gamma}_{\mathbf{k}}. \quad (22)$$

We have eliminated h_x using Eq. (7). The structure factors are given by

$$\gamma_{\mathbf{k}} = \frac{1}{3} \left(\cos k_x + 2 \cos \frac{k_x}{2} \cos \frac{\sqrt{3}k_y}{2} \right), \quad (23)$$

$$\bar{\gamma}_{\mathbf{k}} = \frac{1}{3} \left(\cos \sqrt{3}k_y + 2 \cos \frac{3k_x}{2} \cos \frac{\sqrt{3}k_y}{2} \right). \quad (24)$$

Excitation spectra. We now investigate the nature of the energy spectra of Eq. (2). We will be interested in half-filling or zero magnetic fields and spin-1/2. We adopt the Brillouin zone paths of Refs. [11,12] as shown in Fig. (1). Our main focus is the appearance of a minimum inside the Brillouin zone (roton minimum) and the possibility of any soft modes. The vanishing of the spectrum at the corners of the Brillouin zone represents a phase transition to a new spin configuration. The simplest case is the Heisenberg point $h_{x,z} = J'_z = 0$; $J_z = J_{\pm\pm} = J$. In this limit spin wave theory is exact and the excitation spectrum of Eq. (3) is $\omega_{\mathbf{k}} = A_{\mathbf{k}} = 3J(1 + \gamma_{\mathbf{k}})$, where $B_{\mathbf{k}} = 0$. We see that the exact ground state is the fully polarized easy-axis ferromagnet along the x -axis, and the corresponding excitation exhibits no zero modes since $-1/2 \leq \gamma_{\mathbf{k}} \leq 1$; see Fig. (2). Near $\mathbf{k} = 0$, the energy behaves as $\omega_{\mathbf{k}} \approx a - b\mathbf{k}^2$, with $a = 6J$ and $b = 3J/4$. Hence, the average spin deviation operator near this mode at low-temperature is given by

$$\Delta S_x(T) = \int \frac{d\mathbf{k}}{e^{\omega_{\mathbf{k}}/k_B T} - 1} \sim T \frac{\ln(1 - e^{-a})}{b}. \quad (25)$$

This unusual feature means that the discrete Z_2 symmetry is spontaneously broken even at finite temperature, thus Mermin-Wagner theorem¹⁹ does not apply. Another important feature of Eq. (25) is that we can suppress quantum fluctuations by making the gap “ a ” as large as possible.

As depicted in Figs. (2) and (3), the energy spectra of the Z_2 -invariant XXZ model have a similar behaviour to the $U(1)$ -invariant XXZ model^{11,12} at the corners of the Brillouin zone and along RM except for the case of XY model. At the corners of the Brillouin zone, the spectrum vanishes when $J'_z = J_{\pm\pm} - J_z/2$. Hence at $J'_z = 0$, the transition from the easy-axis ferromagnet to a *ferrosolid* occurs at $J_{\pm\pm} - J_z/2 = 0$, which happens to be the same as the $U(1)$ -invariant model.⁶ As

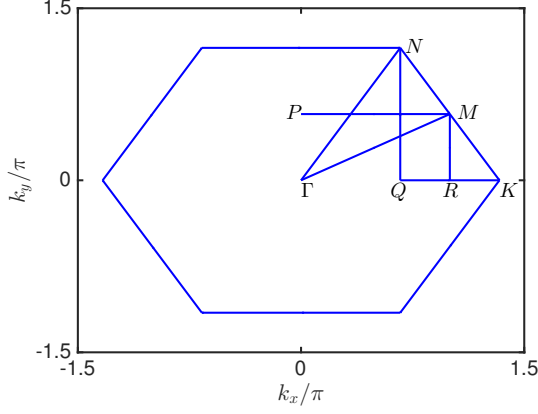


FIG. 1: Color online. The Brillouin zone of the triangular lattice and the corresponding paths that will be adopted in this paper.

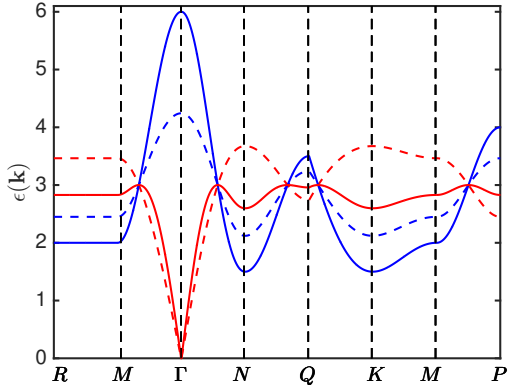


FIG. 2: Color online. The plots of the energy dispersion at $h_{x,z} = 0$ ($\rho = 0.5$) and $J_{\pm\pm} = 1$; $J'_z = 0$. XY model: $J_z = 0$ (dashed). Heisenberg model: $J_z = 1$ (solid). The blue curves denote the present model and the red curves denote the U(1) model.

we will show in the subsequent section, spin wave theory gives a better description of the present model. In contrast to the U(1)-invariant model, the spectra of the Z_2 -invariant model is invariably gapped in the entire Brillouin zone and the spectra display a maxon dispersion at the Γ point ($\mathbf{k} = 0$) as opposed to the usual phonon dispersion in rotational invariant systems. The gapped nature of the Z_2 -invariant model is as a consequence of the Z_2 -symmetry of the Hamiltonian and it plays a very crucial role in the quantum phase diagram of the *Quantum Kagome Ice* uncovered by QMC.^{5,13} The contribution from the $\mathbf{k} = 0$ mode is the most important feature of the Z_2 -invariant model. The gap at the Γ point behaves as $\Delta \propto \sqrt{J_{\pm\pm}(J_z + J'_z + J_{\pm\pm})}$, which vanishes only for $J_{\pm\pm} = 0$. In the subsequent section, we will show that the $\mathbf{k} = 0$ mode enhances the estimated values of the thermodynamic quantities. These trends are

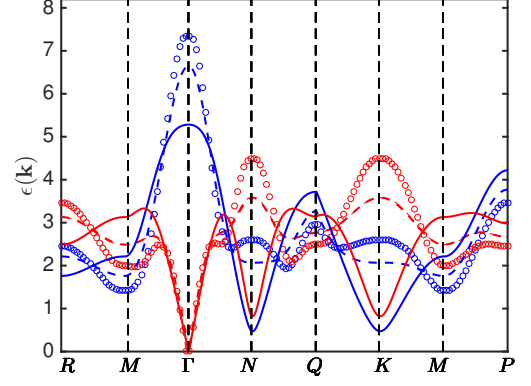


FIG. 3: Color online. The plots of the energy dispersion at $h_{x,z} = 0$ ($\rho = 0.5$), $J_{\pm\pm} = J_z = 1$ and several values of $J'_z = 0.45$ (dashed), $J'_z = -0.45$ (solid), and $J'_z = 1$ (symbol). The colors have the same meaning as in Fig. (2).

slightly modified away from half-filling.

Thermodynamic quantities— The effects of the gapped excitations in the preceding section are manifested explicitly in the ground state thermodynamic quantities. We compute the magnetizations per site given by^{20,21}

$$\langle S_z \rangle = -\frac{1}{SN} \frac{\partial \mathcal{E}_{SW}(\vartheta_0)}{\partial h_z}, \quad (26)$$

$$\langle S_x \rangle = -\frac{1}{SN} \frac{\partial \mathcal{E}_{SW}(\vartheta)}{\partial h_x} \Big|_{\vartheta=\vartheta_0}. \quad (27)$$

Using Eq. (17) we obtain

$$\langle S_z \rangle = S \cos \vartheta_0 + \frac{\cos \vartheta_0}{2\Theta_0} \frac{1}{N} \sum_{\mathbf{k}} \Theta_{\mathbf{k}} \sqrt{\frac{A_{\mathbf{k}}(\vartheta_0) - B_{\mathbf{k}}(\vartheta_0)}{A_{\mathbf{k}}(\vartheta_0) + B_{\mathbf{k}}(\vartheta_0)}}. \quad (28)$$

with $\Theta_{\mathbf{k}} = (J_z + J_{\pm\pm})\gamma_{\mathbf{k}} + J'_z \tilde{\gamma}_{\mathbf{k}}$. The total density of particles is given by $\rho = S + \langle S_z \rangle$. To linear order in h_x we find

$$\langle S_x \rangle = S \sin \vartheta_0 - \frac{\cos^2 \vartheta_0}{2\Theta_0 \sin \vartheta_0} \frac{1}{N} \sum_{\mathbf{k}} \Theta_{\mathbf{k}} \sqrt{\frac{A_{\mathbf{k}}(\vartheta_0) - B_{\mathbf{k}}(\vartheta_0)}{A_{\mathbf{k}}(\vartheta_0) + B_{\mathbf{k}}(\vartheta_0)}} \quad (29)$$

$$- \frac{1}{2 \sin \vartheta_0} \frac{1}{N} \sum_{\mathbf{k}} \left[\frac{A_{\mathbf{k}}(\vartheta_0)}{\omega_{\mathbf{k}}(\vartheta_0)} - 1 \right].$$

Similar to the U(1)-invariant model, the condensate fraction at $\mathbf{k} = 0$ is related to the S_x -order parameter by $\rho_0 = \lim_{S \rightarrow 1/2} \langle S_x \rangle^2$. To linear order in spin wave theory ρ_0 is given by

$$\rho_0 = \rho_0^c - \frac{\cos^2 \vartheta_0}{2\Theta_0} \frac{1}{N} \sum_{\mathbf{k}} \Theta_{\mathbf{k}} \sqrt{\frac{A_{\mathbf{k}}(\vartheta_0) - B_{\mathbf{k}}(\vartheta_0)}{A_{\mathbf{k}}(\vartheta_0) + B_{\mathbf{k}}(\vartheta_0)}} \quad (30)$$

$$- \frac{1}{2} \frac{1}{N} \sum_{\mathbf{k}} \left[\frac{A_{\mathbf{k}}(\vartheta_0)}{\omega_{\mathbf{k}}(\vartheta_0)} - 1 \right].$$

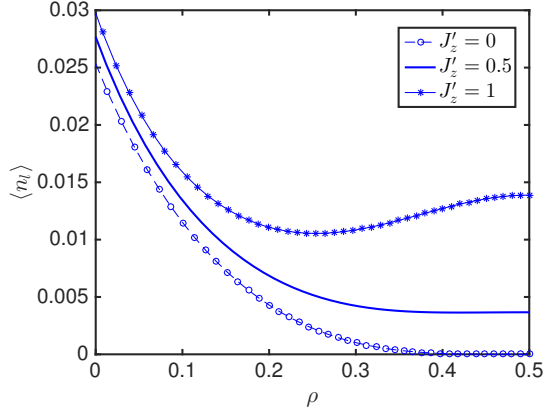


FIG. 4: Color online. The spin-deviation operator against the particle density at $h_x = 0$, $J_{\pm\pm} = J_z = 1$.

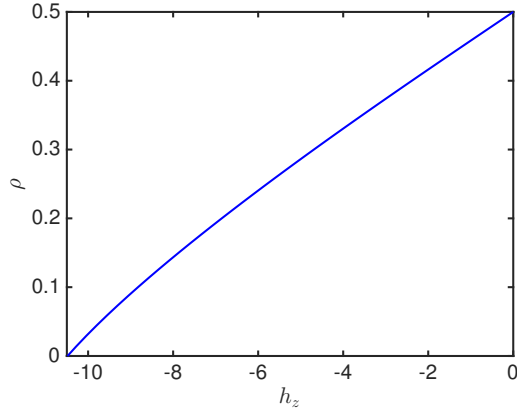


FIG. 5: Color online. The particle density ρ vs. h_z at $J_z = J_{\pm\pm} = 1$, $J'_z = 0$, and $S = 1/2$.

where $\rho_0^c = \frac{1}{4} \sin^2 \vartheta_0$ is the classical condensate fraction. An important feature of the Z_2 -invariant model is that all the thermodynamic quantities are finite at all points in the Brillouin zone. This enhances the estimated values of the thermodynamic quantities. At the XY point, $J_z = J'_z = h_{x,z} = 0$, the estimated value of the order parameter is $\langle S_x \rangle = S - 0.00981$,¹⁵ which should be compared to the O(2)-invariant model $\langle S_x \rangle = S - 0.05146$.²² We see that quantum fluctuations are suppressed in the Z_2 -invariant model. A detail analysis of the XY model has been given elsewhere for the triangular and the kagome lattices.¹⁵ As we can see from Fig. (4), the spin-deviation operator $\langle n_l \rangle$ is extremely small close to half-filling and also very small away from half-filling. In other words, linear spin theory is very suitable for describing the ground state properties of the Z_2 -invariant XXZ model on non-bipartite lattices.¹³⁻¹⁵ We have shown the trend of the particle density in Fig. (5) as a function of h_z . In Fig. (6), we plot the condensate fraction at $\mathbf{k} = 0$ as a function of ρ . At $\rho = 0.5$, the estimated values of ρ_0 at the XY point are $\rho_0 = 0.2402$ linear spin wave

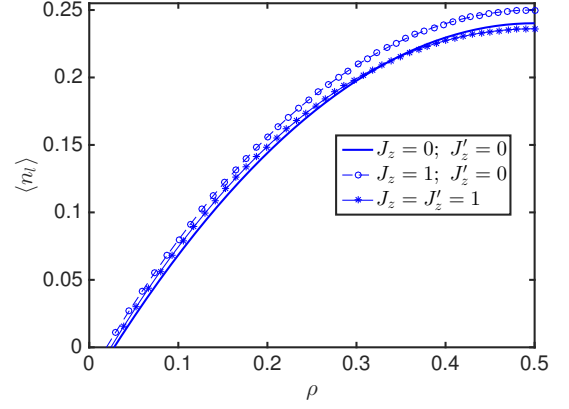


FIG. 6: Color online. The condensate fraction, ρ_0 , against the particle density ρ at $J_{\pm\pm} = 1$ and $S = 1/2$.

theory of the Z_2 -invariant model,¹⁵ $\rho_0 = 0.2011$ series expansion of the O(2)-invariant model,²² and $\rho_0 = 0.19127$ second-order spin wave theory on the square lattice.²¹ At the Heisenberg point, $\rho_0 = \rho_0^c = 0.25$ as expected.

Structure factors— Due to the gapped nature of the Z_2 -invariant model, all the thermodynamic quantities behave nicely without any divergent contributions. The density of states for this model is depicted in Fig. (7) for several values of the anisotropies. There are some striking features in the density of states of this model. We observe several spikes (van Hove singularities) depending on the anisotropies, which stem from the $\mathbf{k} = 0$ mode and the flat mode along RM . In the case of XY model, the major contribution to the spike comes from the $\mathbf{k} = 0$ mode and the discontinuity is a result of the lowest energy states at the roton minima at the corners of the Brillouin zone.

Let us turn to the calculation of the dynamical structure factors, which is given by

$$S^{\beta\gamma}(\mathbf{k}, \omega) = \frac{1}{2\pi} \int_{-\infty}^{\infty} dt e^{i\omega t} \langle S_{\mathbf{k}}^{\beta}(t) S_{-\mathbf{k}}^{\gamma}(0) \rangle, \quad (31)$$

where $S_{\mathbf{k}}^{\beta} = \frac{1}{\sqrt{N}} \sum_l e^{-i\mathbf{k}l} S_l^{\beta}$ is the Fourier transform of the operators, and $\beta, \gamma = (x, y, z)$ label the components of the spins. At zero temperature, the structure factors are obtained from the Green's function:

$$S^{\beta\gamma}(\mathbf{k}, \omega) = -\frac{1}{\pi} \text{Im } \mathcal{G}^{\beta\gamma}(\mathbf{k}, \omega), \quad (32)$$

with $\mathcal{G}^{\beta\gamma}(\mathbf{k}, \omega) = -i \langle T S_{\mathbf{k}}^{\beta}(t) S_{-\mathbf{k}}^{\gamma}(0) \rangle$ being the time-ordered retarded Green's function. At half-filling or zero magnetic fields, $\theta = \pi/2$, Eq. (11) gives $S_l^x \rightarrow S_l'^z$ and $S_l^z \rightarrow -S_l'^x$. The quantization axis in this case is along the x -axis and the off-diagonal terms are $S_l^{\pm} = S_l^z \pm i S_l^y$. Using linear spin wave theory to order S we find the two static structure factors at half-filling: $S^{zz}(\mathbf{k}) = S(u_{\mathbf{k}} - v_{\mathbf{k}})^2/2$ and $S^{\pm}(\mathbf{k}) = 2Sv_{\mathbf{k}}^2$. The static structure factors $S^{zz}(\mathbf{k})$ and $S^{\pm}(\mathbf{k})$ are shown in Figs. (8) and (9) respectively. In contrast to the $U(1)$ -invariant model, the

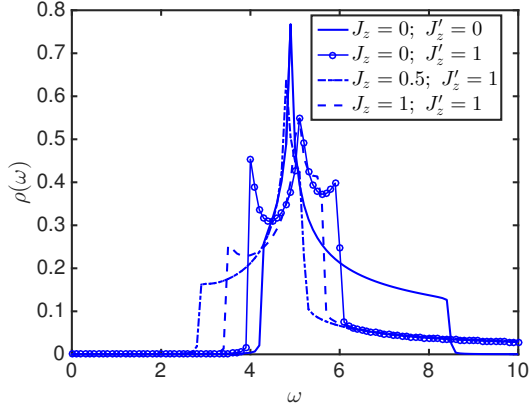


FIG. 7: Color online. The density of states $D(\omega)$ vs. ω at half-filling, $h_{x,z} = 0$ ($\rho = 0.5$); $J_{\pm\pm} = J'_z = 1$.

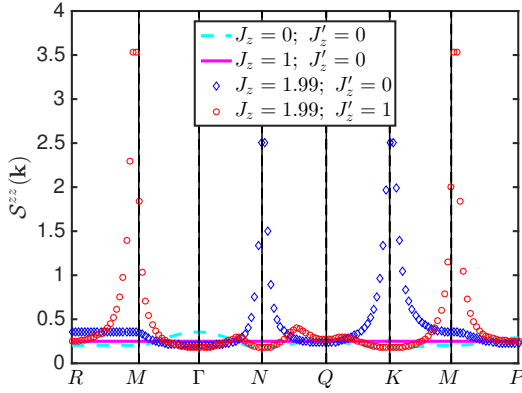


FIG. 8: Color online. The static dynamical structure factor, $S^{zz}(\mathbf{k})$, along the Brillouin zone paths in Fig. (1) at $h_{x,z} = 0$ ($\rho = 0.5$); $J_{\pm\pm} = 1$ and $S = 1/2$.

static structure factors show no discontinuity in the entire Brillouin zone. Our calculation shows that $S^{zz}(\mathbf{k})$ develops sharp step-like peaks at the minima of the energy spectra and it is completely flat at the Heisenberg point $J_{\pm\pm} = J_z = 1$, $J'_z = 0$. The off-diagonal term $S^{\pm}(\mathbf{k})$ exhibits a similar behaviour but become completely zero except at the peaks. At $K = \mathbf{Q} = (\pm 4\pi/3, 0)$ we find

$$S(\mathbf{Q}) = \frac{S}{2} \sqrt{\frac{J_{\pm\pm}}{2(J_{\pm\pm} + J'_z) - J_z}}. \quad (33)$$

Figure (10) shows the plot of $S(\mathbf{Q})$ as a function of J_z .

Conclusion–. We have explored the ground state thermodynamic properties of the easy-axis ferromagnetic phase of the quantum triangular ice model. We observed fascinating features which are different from the U(1)-invariant XXZ model. In particular, divergent and discontinuous quantities in the U(1)-invariant XXZ model are finite in the Z_2 -invariant XXZ model, hence all the points in the Brillouin zone contribute to the thermo-

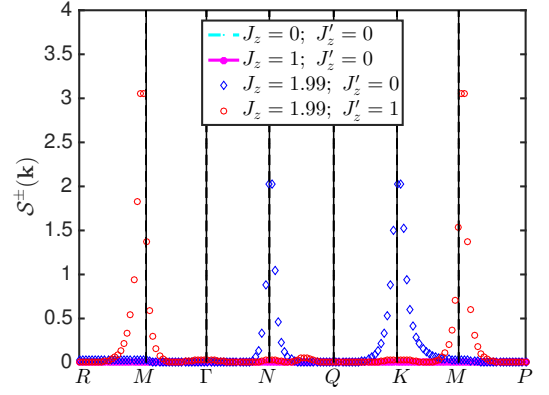


FIG. 9: Color online. The static dynamical structure factor, $S^{\pm}(\mathbf{k})$, along the Brillouin zone paths in Fig. (1). The parameter are the same as in Fig. (8).

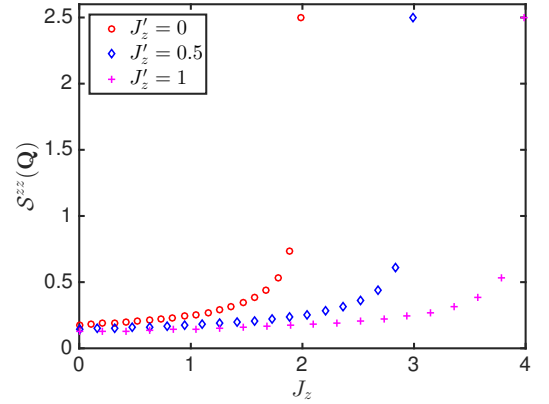


FIG. 10: Color online. The static structure factor, $S^{zz}(\mathbf{Q})$ as a function of J_z at $J_{\pm\pm} = 1$.

dynamic quantities. Interestingly, we found that linear spin wave theory provides an accurate picture of this system with the spin-deviation operator $\langle n_l \rangle < 0.025$ for all parameter regimes considered. In contrast to rotational invariant systems, at the Heisenberg point, the ferromagnetic state of the Z_2 -invariant model exhibits no Goldstone mode at $\mathbf{k} = 0$. The excitation spectrum is gapped in the entire Brillouin zone, and the average spin-deviation is finite at low temperature near the gapped states. Hence, the Z_2 discrete symmetry is spontaneously broken even at finite temperature. As a result of the distinctive features of this model, the particle density and the condensate fraction at half-filling give reasonable estimates at the level of our spin wave theory. Also, the dynamical structure factors and the density of states exhibit interesting peaks at unusual momenta. The most distinctive feature of the Z_2 -invariant model comes from the $\mathbf{k} = 0$ mode. This mode plays a very prominent role in the unconventional phases obtained from the fully frustrated Z_2 -invariant model.^{5,13} The features uncovered in

this paper might be useful for experimental purposes in gapped physical systems that could be modeled with the Z_2 -invariant model. It is also interesting to investigate the nature of this model in quantum optical lattices.^{17,18} An investigation of magnon decay would be of interest in the Z_2 -invariant model, this requires one to go beyond the linear spin wave approximation; however, this is not very important at the level of our investigation since lin-

ear spin wave theory provides reasonable estimates of the thermodynamic quantities.

Acknowledgments—The author would like to thank African Institute for Mathematical Sciences (AIMS), where this work was conducted. Research at Perimeter Institute is supported by the Government of Canada through Industry Canada and by the Province of Ontario through the Ministry of Research and Innovation.

-
- * Electronic address: solomon@aims.ac.za
† Electronic address: sowerre@perimeterinstitute.ca
- ¹ Gingras, M. J. P. and McClarty, P. A., Reports on Progress in Physics **77**, 056501 (2014).
 - ² Zhihao Hao, Alexandre G. R. Day, and Michel J. P. Gingras, Phys. Rev. B **90**, 214430, (2014).
 - ³ Lucile Savary and Leon Balents, Phys. Rev. Lett. **108**, 037202, (2012).
 - ⁴ Huang, Y.-P., Chen, G. and Hermele, M. Phys. Rev. Lett. **112**, 167203 (2014).
 - ⁵ Juan Carrasquilla, Zhihao Hao, and Roger G. Melko, Nature Communications, **6**, 7421, (2015).
 - ⁶ Ganpathy Murthy, Daniel Arovas, and Assa Auerbach, Phys. Rev. B **55**, 3104, (1997).
 - ⁷ Heidarian D and Damle K, Phys. Rev. Lett. **95**, 127206, (2005).
 - ⁸ Stefan Wessel and Matthias Troyer, Phys. Rev. Lett. **95**, 127205, 2005.
 - ⁹ Melko R G, *et. al*, Phys. Rev. Lett. **95**, 127207, 2005.
 - ¹⁰ S. V. Isakov, *et. al*, Phys. Rev. Lett. **97**, 147202, 2006.
 - ¹¹ Tyler Bryant and Rajiv R. P. Singh, Phys. Rev. B , **76**, 064520, (2007).
 - ¹² T. N. Antsygina, *et. al*, Phys. Rev. B , **82**, 144504, (2010).
 - ¹³ S. A. Owerre, A.A. Burkov, and Roger G. Melko. (To be published).
 - ¹⁴ S. A. Owerre, arXiv:1511.01843 [cond-mat.str-el].
 - ¹⁵ S. A. Owerre, (To be published).
 - ¹⁶ A Galatanu *et. al*, J. Phys.: Condens. Matter **15**, S2187, (2003); S. Raymond *et. al*, Phys. Rev. B **82**, 094416, (2010).
 - ¹⁷ Markus Greiner *et. al*, Nature, **415**, 39, (2002).
 - ¹⁸ C Becker *et. al*, New Journal of Physics, **12**, 065025, (2010).
 - ¹⁹ Mermin, N. D. and Wagner, H., Phys. Rev. Lett. , **17**, 1133, (1966).
 - ²⁰ K. Bernardet *et. al*, Phys. Rev. B **65**, 104519 (2002).
 - ²¹ Tommaso Coletta, Nicolas Laflorencie, and Frédéric Mila, Phys. Rev. B **85**, 104421 (2012).
 - ²² Zheng Weihong, J. Oitmaa, and C. J. Hamer, Phys. Rev. B **44**, 11869, 1991.